Higgs boson decays in the Complex MSSM

Karina Williams[1] [a] and Georg Weiglein[1] [b]

IPPP, University of Durham, Durham DH1 3LE, UK

Abstract. The analysis of the Higgs search results at LEP showed that a part of the MSSM parameter space with non-zero complex phases could not be excluded, where the lightest neutral Higgs boson, h_1, has a mass of only about 45 GeV and the second lightest neutral Higgs boson, h_2, has a sizable branching fraction into a pair of h_1 states. Full one-loop results for the Higgs cascade decay $h_2 \to h_1 h_1$ are presented and combined with two-loop Higgs propagator corrections taken from the program *FeynHiggs*. Using the improved theoretical prediction to analyse the limits on topological cross sections obtained at LEP, the existence of an unexcluded region at low Higgs mass is confirmed. The effect of the genuine vertex corrections on the size and shape of this region is discussed.

PACS. 12.60.Jv Supersymmetric models – 14.80.Cp Non-standard-model Higgs bosons

1 Introduction

In its general form, the MSSM contains complex phases which drive $\mathcal{CP}$-violation. The results of the Higgs-boson searches at LEP were analysed in a series of MSSM benchmark scenarios [1, 2], including one explicitly chosen to investigate the effects of these $\mathcal{CP}$-violating phases, called the CPX scenario [2]. This scenario produced an unexcluded region for light h_1 and relatively small values of $\tan\beta$ (the ratio of the vacuum expectation values of the two Higgs doublets), so that no firm lower bound on the mass of the lightest Higgs boson of the MSSM could be set [3]. Throughout much of this region of CPX parameter space, the process $h_2 \to h_1 h_1$ dominates the h_2 decay width. Therefore, in order to reliably determine which parameter regions of the MSSM are unexcluded by the Higgs searches so far and which regions will be accessible by Higgs searches in the future, precise predictions for this process are indispensable.

However, the genuine vertex corrections (as opposed to propagator corrections) to the process $h_2 \to h_1 h_1$ in the MSSM with complex parameters have so far been unavailable within the Feynman-diagrammatic (FD) approach. These vertex corrections are expected to be sizable as they contain terms depending on the fourth power of the top mass. We have obtained complete one-loop results within the FD approach for the decays $h_a \to h_b h_c$, including all genuine one-loop vertex corrections, in the MSSM with complex phases (cMSSM) [4]. We have furthermore calculated complete one-loop results for the decays of neutral Higgs bosons into SM fermions in the cMSSM [4]. These new one-loop results are combined with existing higher-order corrections in the FD approach and will be included in the public code *FeynHiggs* [5–8]. As an application of our improved result, we analyse the coverage of the LEP exclusion limits on the topological cross sections for the various Higgs-boson production and decay cross sections within the M_{h_1}–$\tan\beta$ parameter plane.

2 Calculation of Higgs-boson cascade decays and decays into SM fermions

We calculated the full 1PI (one-particle irreducible) one-loop vertex contributions to the processes $h_a \to h_b h_c$, taking into account all sectors of the MSSM and the complete dependence on the complex phases of the supersymmetric parameters. These calculations (which make use of the programs *FeynArts* [9] and *FormCalc* [10]) have been described in more detail in Ref. [4].

We have derived also complete one-loop results for the processes $h_a \to f\bar{f}$ (including SM-type QED and, where appropriate, QCD corrections) for arbitrary values of all complex phases of the supersymmetric parameters, as these decays are important over large parts of the cMSSM parameter space. The partial decay widths for the other Higgs-boson decay modes have been taken from the program *FeynHiggs*.

In our numerical analysis below, we will compare our full result with the contribution from just the $t, \tilde{t}$ sector in the approximation where the gauge couplings are neglected and the diagrams are evaluated at zero external momenta, which we call the 'Yukawa Approximation'.

[a] *Email: k.e.williams@durham.ac.uk*
[b] *Email: georg.weiglein@durham.ac.uk*

For the renormalisation of the Higgs fields it is convenient to use a $\overline{\rm DR}$ scheme as in Ref. [5]. Therefore, it is necessary to include finite wave-function normalisation factors (Z-factors) to ensure that S-matrix elements involving external Higgs fields have the correct on-shell properties. The form of these Z-factors is given in Ref. [4]. In the calculation of the Z-factors, we incorporate higher-order contributions obtained from the neutral Higgs-boson self-energies of the program *FeynHiggs*. In the analysis below, we will restrict to those higher-order contributions for which the phase dependence at the two-loop is explicitly known [6], i.e. we do not include contributions that have been extrapolated from results obtained for the real MSSM.

3 Implementation of exclusion bounds from the LEP Higgs searches

In our numerical analysis below we analyse the impact of our new result on the LEP exclusion bounds in the cMSSM. This is done by comparing the cMSSM predictions with the topological cross section limits given in Refs. [3, 11]. This procedure is described in more detail in Ref. [4] and Ref. [12]. It involves checking which channel is predicted to have the highest statistical sensitivity and then comparing the theoretical prediction in that channel only with the topological cross section limit determined at LEP. This ensures a correct statistical interpretation of the overall exclusion limit at the 95% C.L.. However, it should be noted that, since only one channel can be used at a time, this method leads to poorer coverage in areas where two or more channels have a similar statistical sensitivity than, for example, the dedicated analyses carried out in Ref. [3].

4 Numerical results

In our numerical analysis we use the parameter values of the CPX benchmark scenario [2], adapted to the latest experimental central value of the top-quark mass [13] and using an on-shell value for the absolute value of the trilinear couplings A_t and A_b that is somewhat shifted compared to the $\overline{\rm DR}$ value specified in Ref. [2]. Specifically, if not indicated differently, we use the parameters

$$\begin{aligned} &M_{\rm SUSY} = 500 \text{ GeV}, \ |A_t| = |A_b| = 900 \text{ GeV}, \\ &\mu = 2000 \text{ GeV}, \ m_{\tilde g} \equiv |M_3| = 1000 \text{ GeV}, \\ &m_t = 170.9 \text{ GeV}, \ M_2 = 200 \text{ GeV}. \end{aligned} \tag{1}$$

The lowest-order Higgs sector parameters $\tan\beta$ and $M_{H^\pm}$ are varied, with $M_{H^\pm} < 1000$. The complex phases of the trilinear couplings A_t, A_b and the gluino mass parameter M_3 are set to

$$\varphi_{A_t} = \frac{\pi}{2}, \quad \varphi_{A_b} = \frac{\pi}{2}, \quad \varphi_{\tilde g} = \frac{\pi}{2}. \tag{2}$$

In Eq. (1) $M_{\rm SUSY}$ denotes the diagonal soft SUSY-breaking parameters in the sfermion mass matrices, which are chosen to be equal to each other.

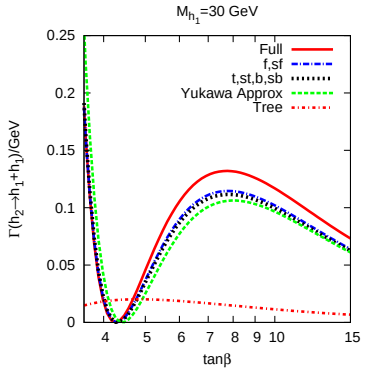

Fig. 1. $\Gamma(h_2 \to h_1 h_1)$ as function of $\tan\beta$ ($M_{H^\pm}$ is adjusted to ensure $M_{h_1} = 30$ GeV), for various approximations.

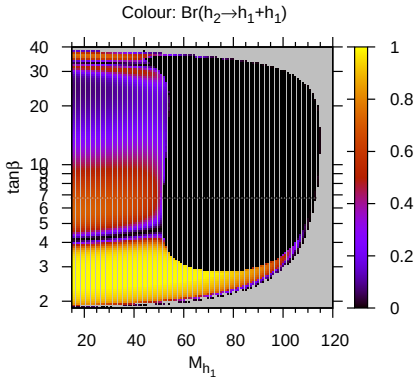

Fig. 2. The branching ratio $\mathrm{BR}(h_2 \to h_1 h_1)$ in the M_{h_1}–$\tan\beta$ plane of the CPX scenario.

4.1 Results for the $h_2 \to h_1 h_1$ decay width

Fig. 1 shows the relative effect of different contributions to the $h_2 \to h_1 h_1$ decay width in an area of the cMSSM parameter space that is particularly relevant to the unexcluded regions in the LEP Higgs searches. The decay width is plotted against $\tan\beta$ whilst adjusting $M_{H^\pm}$ such that $M_{h_1} = 30$ GeV. All the results plotted include the higher-order corrected wave-function normalisation factors as described in Sect. 3. The results differ only in the genuine contributions to the $h_2 h_1 h_1$ vertex. One can see that the full result (denoted as 'Full') differs drastically from the case where only wave-function normalisation factors but no genuine one-loop vertex contributions are taken into account ('Tree'). The Yukawa approximation agrees much better with the full result and explains the qualitative behaviour of the full result — in particular, the region where $\Gamma(h_2 \to h_1 h_1) \approx 0$ for $\tan\beta \approx 4.3$ is due to the fact that the Yukawa vertex corrections to the matrix element change sign when $\tan\beta$ is varied. Using the full contribution from the $t, \tilde t, b, \tilde b$ sector ('t, st, b, sb') or using all three generations of fermions and sfermions ('f, sf') yields a prediction that deviates from the full result by up to 15%.

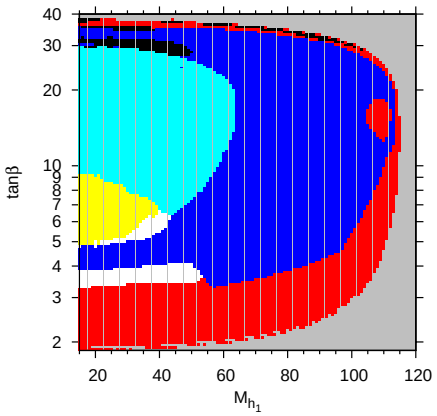

Fig. 3. The channels predicted to have the highest statistical sensitivity for setting an exclusion limit using the results from the LEP Higgs searches in the CPX scenario. The colour codings are: red = $(h_1Z) \to (b\bar{b}Z)$, blue = $(h_2Z) \to (b\bar{b}Z)$, white = $(h_2Z) \to (h_1h_1Z) \to (b\bar{b}b\bar{b}Z)$, cyan = $(h_2h_1) \to (b\bar{b}b\bar{b})$, yellow = $(h_2h_1) \to (h_1h_1h_1) \to (b\bar{b}b\bar{b}b\bar{b})$, black = other channels.

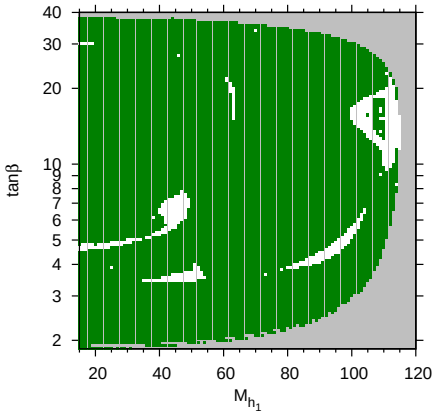

Fig. 4. The parameter regions in the CPX scenario excluded at the 95% C.L. by the topological cross section limits obtained at LEP [3]. The colour codings are: green = LEP excluded, white = LEP allowed, grey = theoretically inaccessible.

In Figs. 2, 3 and 4 the M_{h_1}–$\tan\beta$ parameter space of the CPX scenario is analysed. Fig. 2 shows the branching ratio of the Higgs cascade decay, $\mathrm{BR}(h_2 \to h_1h_1)$. Over a large part of the parameter space where the decay $h_2 \to h_1h_1$ is kinematically possible it is actually the dominant decay channel. The branching ratio is particularly large for low and moderate values of $\tan\beta$. In the region where $\tan\beta \approx 4$–5 the Yukawa contribution to the matrix element for the $h_2 \to h_1h_1$ decay changes sign and causes a sharp drop in the $h_2 \to h_1h_1$ branching ratio, as was already observed in Fig. 1. A similar behaviour occurs also in the region of $\tan\beta \approx 35$.

Fig. 3 indicates which channel has the highest statistical sensitivity and therefore which channel will be used to set an exclusion limit in different regions of the parameter space. As explained in Sect. 4, this information is needed for a statistical interpretation of the topological cross section limits obtained at LEP. One can see in the figure that the channels $e^+e^- \to h_2Z \to h_1h_1Z \to b\bar{b}b\bar{b}Z$ and $e^+e^- \to h_2h_1 \to h_1h_1h_1 \to b\bar{b}b\bar{b}b\bar{b}$ have the highest search sensitivity in a region with small M_{h_1} and small and moderate values of $\tan\beta$ (the region at $\tan\beta \approx 4$ where the channel $e^+e^- \to (h_2Z) \to (b\bar{b}Z)$ has the highest search sensitivity corresponds to the drop in the $h_2 \to h_1h_1$ branching ratio observed in Fig. 2). For small M_{h_1} and somewhat higher $\tan\beta$ the channel $e^+e^- \to (h_2h_1) \to (b\bar{b}b\bar{b})$ has the highest search sensitivity. It should be noted that all channels involving the decay of the h_2 boson in the region of small M_{h_1} are strongly influenced by the $\Gamma(h_2 \to h_1h_1)$ decay width, either directly in the case of the channels involving the Higgs cascade decay, or indirectly through the branching ratio of the h_2. The parameter region where $\Gamma(h_2 \to h_1h_1)$ is important coincides with the region of the CPX scenario that could not be excluded at the 95% C.L. in the analysis of the four LEP collaborations [3].

In Fig. 4 we have compared our new theoretical predictions with the topological cross section limits obtained at LEP for the channels in Fig. 3. We find two unexcluded regions at $M_{h_1} \approx 45$ GeV and moderate $\tan\beta$ where channels involving the decay $h_2 \to h_1h_1$ play an important role. Thus, our analysis, based on the most up-to-date theory prediction for the $h_2 \to h_1h_1$ channel, confirms the 'hole' in the LEP coverage observed in Ref. [3] (see in particular Fig. 19 of Ref. [3]).

It should be noted, on the other hand, that the results shown in Fig. 4 differ in several respects from the results presented in Ref. [3]. Most notable are several small unexcluded regions in our plot that were not present in the results of Ref. [3]. By comparison with Fig. 3, one can see that the unexcluded regions occur on borders between areas where different search topologies are predicted to have the highest exclusion power. As discussed above, our analysis has less statistical sensitivity in these border regions than the benchmark studies of Ref. [3]. A further difference (besides the improved theoretical prediction) is the input value of the top-quark mass. While we are using the latest experimental central value of $m_t = 170.9$ [13], most of the analysis of Ref. [3] was done for $m_t = 174.3$. We have explicitly checked that (as expected) the unexcluded regions are significantly increased if we use $m_t = 174.3$ instead. It should also be noted that the shape and size of the unexcluded regions depend sensitively on the value of A_t used.

In Fig. 5 we focus on the parameter region at $M_{h_1} \approx 45$ GeV and moderate $\tan\beta$. While plot (a) shows the full result (i.e., it is a detailed view of Fig. 4), in plot (b) the genuine $h_2 \to h_1h_1$ vertex corrections are approximated by the contributions from fermions and sfermions only, and in plot (c) the Yukawa Approximation has been used for the genuine $h_2 \to h_1h_1$ vertex corrections. In all three plots the wave function normalisation factors and all other decay widths are the

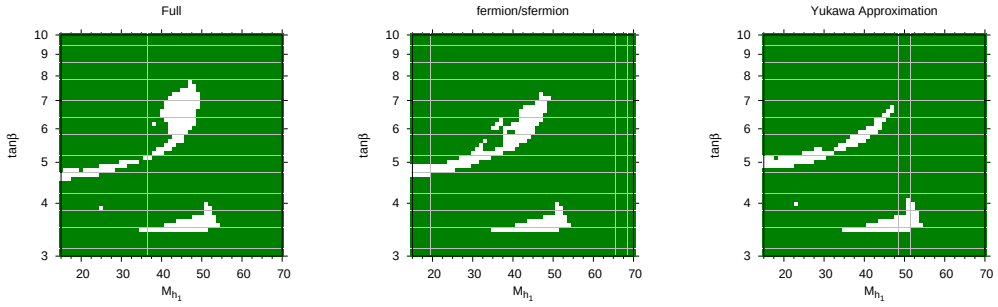

(a) (b) (c)

Fig. 5. A closer look at the LEP coverage for $M_{h_1} \approx 45$ GeV and moderate $\tan\beta$. Plot (a) shows the full result (detailed view of plot (b) of Fig. 3). Plot (b) shows the result for the case where only contributions from SM fermions and their superpartners are taken into account in the genuine vertex corrections. Plot (c) shows the result where the Yukawa Approximation has been used for the genuine vertex corrections. The colour codings are: green = LEP excluded, white = LEP allowed.

same. While all three graphs show unexcluded regions in similar positions in parameter space, the shape of the unexcluded region at $M_{h_1} \approx 45$ GeV and $\tan\beta \approx 6$ changes quite significantly.

5 Conclusions

We have shown that our new result for the decay width $h_2 \to h_1 h_1$, which includes the complete one-loop vertex corrections, drastically improves on results obtained using propagator corrections alone. We have combined this with new results for neutral Higgs decays into two fermions in order to re-analyse the CPX parameter space using the limits on topological cross sections obtained from the LEP Higgs searches. We find that over a large part of the parameter space where the decay $h_2 \to h_1 h_1$ is kinematically possible, it is the dominant decay channel. We confirm that the parameter space at low Higgs mass can not be completely excluded by the LEP Higgs searches. We furthermore show that the size and shape of the unexcluded regions are significantly modified if approximations to the full result are used, emphasizing the relevance of the full one-loop result for the $h_2 \to h_1 h_1$ decay width in the complex MSSM.

Acknowledgements

We are grateful to P. Bechtle, O. Brein, T. Hahn, S. Heinemeyer, W. Hollik, S. Palmer, H. Rzehak and D. Stöckinger for many helpful discussions. Work supported in part by the European Community's Marie-Curie Research Training Network under contract MRTN-CT-2006-035505 'Tools and Precision Calculations for Physics Discoveries at Colliders'.

References

1. M. Carena, S. Heinemeyer, C. Wagner and G. Weiglein, hep-ph/9912223; *Eur. Phys. J.* **C 26** (2003) 601, hep-ph/0202167.
2. M. Carena, J. Ellis, A. Pilaftsis and C. Wagner, *Phys. Lett.* **495** (2000) 155, hep-ph/0009212.
3. [LEP Higgs working group], *Phys. Lett.* **B 565** (2003) 61, hep-ex/0306033; *Eur. Phys. J.* **C 47** (2006) 547, hep-ex/0602042.
4. K.E. Williams and G. Weiglein, arXiv:0710.5320 [hep-ph].
5. M. Frank, T. Hahn, S. Heinemeyer, W. Hollik, H. Rzehak and G. Weiglein, *JHEP* **02** (2007) 047, hep-ph/0611326.
6. S. Heinemeyer, W. Hollik, H. Rzehak and G. Weiglein, *Phys. Lett.* **B 652** (2007) 300, arXiv:0705.0746 [hep-ph].
7. S. Heinemeyer, W. Hollik and G. Weiglein, *Phys. Rev.* **D 58** (1998) 091701, hep-ph/9803277; *Phys. Lett.* **B 440** (1998) 296, hep-ph/9807423; *Eur. Phys. J.* **C 9** (1999) 343. hep-ph/9812472;
   M. Frank, S. Heinemeyer, W. Hollik and G. Weiglein, hep-ph/0212037, in the proceedings of *SUSY02*, July 2002, DESY, Hamburg, Germany;
   G. Degrassi, S. Heinemeyer, W. Hollik, P. Slavich and G. Weiglein, *Eur. Phys. J.* **C 28** (2003) 133, hep-ph/0212020.
8. S. Heinemeyer, W. Hollik and G. Weiglein, *Comput. Phys. Commun.* **124** (2000) 76, hep-ph/9812320; hep-ph/0002213; see `www.feynhiggs.de` .
9. J. Küblbeck, M. Böhm and A. Denner, *Comput. Phys. Commun.* **60** (1990) 165;
   T. Hahn, *Comput. Phys. Commun.* **140** (2001) 418, hep-ph/0012260;
   T. Hahn and C. Schappacher, *Comput. Phys. Commun.* **143** (2002) 54, hep-ph/0105349.
   The program and the user's guide are available via `www.feynarts.de` .
10. T. Hahn and M. Pérez-Victoria, *Comput. Phys. Commun.* **118** (1999) 153, hep-ph/9807565.
11. P. Bechtle, private communication.
12. P. Bechtle et al., in preparation.
13. Tevatron Electroweak Working Group, hep-ex/0703034.